

hours after inoculation of the bacteria, animals developed signs of infection – lethargy, decreased food intake, piloerection and ruffled fur. Histological analysis showed a marked diffuse infiltration of neutrophils in the lungs of infected animals. Many neutrophils were found in the alveolar spaces and occasional neutrophil aggregates were observed. In addition, there was diffuse hyperaemia and scattered areas of haemorrhage (data not shown). Within the time frame of the experiment (48 h) and when compared to uninfected mice, there did not seem to be an increase in the number of mononuclear cells in lung tissues (data not shown). In order to quantify the influx of neutrophils into the lungs of infected animals, we assessed the number of neutrophils (PMN) in BAL fluid and tissue MPO activity. In BAL fluid, there was an accumulation of PMN that was substantial at 24 h and was sustained until 48 h after infection (Figure 1A). Similarly, there was a marked infiltration of neutrophils in the lung parenchyma, as assessed by tissue MPO activity (Figure 1B). Neutrophils were first observed at 24 h after infection and greater numbers were observed after 48 h (Figure 1B). With an exception of a neutrophilia observed at 2.5 h, there were few modifications in total or differential leukocyte counts in blood (data not shown).

The concentration of bacteria in the lungs of infected mice rapidly increased after the inoculation of *K. pneumoniae* (Figure 2). The total number of bacteria was already greater than 1×10^8 CFU per lung 2.5 h after infection. These concentrations increased rapidly and were not countable at 48 h at the dilutions used (Figure 2). In contrast, we failed to observe any dissemination of the infection, as no *K. pneumoniae* colony could be determined in plasma in any of the time points until 48 h after infection (data not shown).

KC and TNF- α are known to play a role during gram negative bacterial infection in mice (Tsai et al., 1998; Greenberger et al., 1995; Laichalk et al., 1996). Experiments evaluating the kinetics of expression of KC and TNF- α in lung homogenates after *K. pneumoniae* are shown in Figure 3. Markedly elevated concentrations of both cytokines in lungs were already detectable at 2.5 h after infection. The concentrations were still elevated at 24 h and levels started to fall at 48 h (Figure 3). No TNF- α could be detected in plasma samples in any of the time points measured and KC

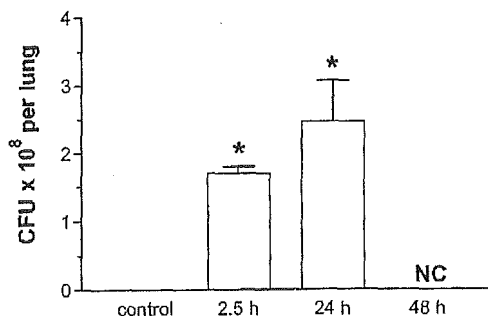


Figure 2 Kinetics of the number of colony-forming units (CFU) in the lungs of mice infected with *K. pneumoniae*. Animals were inoculated with 3×10^6 bacteria or vehicle (30 μ l) and the number of CFU in lung tissue evaluated after 2.5, 24 and 48 h. At 48 h, the number of CFU was not countable (NC). Results are shown as the mean \pm s.e. mean of five animals in each group. * $P < 0.01$ when compared with uninfected animals.

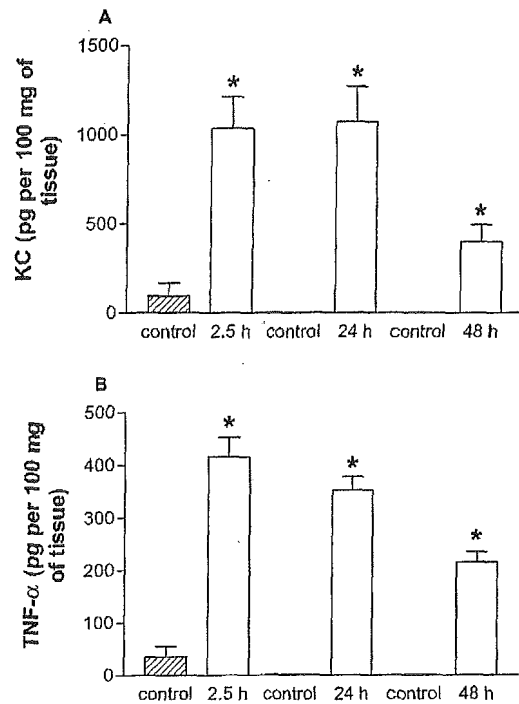


Figure 3 Kinetics of TNF- α and KC protein production in lung homogenates after infection with *K. pneumoniae*. Animals were inoculated with 3×10^6 bacteria or vehicle (30 μ l) and the concentration of KC (A) and TNF- α (B) in lung tissue evaluated by ELISA after 2.5, 24 and 48 h. Results are shown as the mean \pm s.e. mean of six animals in each group. * $P < 0.01$ when compared with uninfected animals.

was detectable in plasma at 2.5 h and 24 h after infection but not at 48 h (control, below detection limit; 2.5 h, 759.35 ± 209.95 pg ml⁻¹; 24 h, 121.4 ± 92.0 pg ml⁻¹; 48 h, below detection limit; $n = 6$). In all further experiments, samples were harvested at 24 h after infection, as tissue inflammation was marked at this time point, bacteria levels in tissues were elevated and all animals were alive but with signs of infection.

Effects of the treatment with the PAF receptor antagonist UK-74,505 on the course of *K. pneumoniae* infection

Treatment with UK-74,505 had no significant effect on the number of neutrophils which were recruited into the airspaces of infected animals (infected animals, $34.0 \pm 17.7 \times 10^5$ neutrophils; infected and UK-74,505-treated, $42.8 \pm 13.7 \times 10^5$, $n = 6$). Similarly, the recruitment of neutrophils in the lung of UK-74,505-treated mice, as assessed by MPO assay (Infected, 1.2 ± 0.2 ; Infected + UK-74,505, $0.9 \pm 0.2 \times 10^6$ neutrophils 100 mg⁻¹ of tissue, $n = 6$), was not significantly different from vehicle-treated *K. pneumoniae*-infected animals. Histological analysis of lungs of infected animals treated with vehicle or UK-74,505 showed a marked diffuse infiltration of neutrophils, hyperaemia and areas of haemorrhage. There did not appear to be any qualitative differences between the two groups (data not shown).

In agreement with the lack of effect of the PAFR antagonist on neutrophil recruitment into the lung tissue, the tissue and BAL fluid concentrations of the neutrophil-

active chemokine KC was not different in UK-74,505-treated and untreated mice (Figure 4A,B). Similarly, pulmonary tissue concentrations of MCP-1 were not significantly different in both groups of animals (Infected, 1516.0 ± 194.0 pg per 100 mg of tissue; infected and UK-74,505-treated, 1129.4 ± 103.4 pg per 100 mg of tissue; $n=6$). In contrast, treatment with UK-74,505 significantly decreased the concentrations of TNF- α detected in the lung and BAL fluid of *K. pneumoniae*-infected mice (Figure 4C,D).

The effects of daily treatment of *K. pneumoniae*-infected mice with UK-74,505 on bacterial counts is shown in Figure 5. Treatment with UK-74,505 resulted in a significant increase in the number of CFU in the lungs of *K. pneumoniae*-infected mice (Figure 5A). Similarly, infection of PAFR^{-/-} mice with *K. pneumoniae* resulted in a larger number of CFU in the lungs when compared to wild-type controls (Figure 5B).

The percentage of BAL neutrophils that had ingested at least one bacterium was evaluated 24 h after infection. As seen in Table 1, pre-treatment with UK-74,505 was accompanied by a 50% inhibition of the ability of BAL neutrophils to phagocytose *K. pneumoniae*. Similarly, there was a marked suppression of *K. pneumoniae* uptake by BAL neutrophils from PAFR^{-/-} mice when compared to their wild type controls (Table 1).

Survival of mice infected with *K. pneumoniae*

Subsequent experiments were performed to examine the contribution of PAF to the survival of mice infected with

K. pneumoniae. As shown in Figure 6, all untreated *K. pneumoniae*-infected animals were alive by 72 h of infection after which time mortality increased substantially, with 100% lethality noted by day 5 after inoculation. The treatment with UK-74,505 resulted in earlier lethality with 30 and 85% of animals dead at 72 and 96 h, respectively (Figure 6). Similarly, infection of PAFR^{-/-} mice with *K. pneumoniae* resulted in significantly earlier lethality when compared to wild-type animals (Figure 6). Of note, 40% of animals were dead at 48 h after infection.

Discussion

The host defence against acute bacterial infection requires the generation of a vigorous inflammatory response that predominantly involves recruitment and activation of neutrophils. Although in the majority of cases this response is sufficient to control infection, an overt inflammatory response may cause marked tissue injury, haemodynamic shock and death (Teixeira *et al.*, 2001). PAF is a biologically active phospholipid mediator known to be important for the ability of leucocytes to phagocytose foreign particles and kill microorganisms (Ishii & Shimizu, 2000; Au *et al.*, 2001). On the other hand, several studies have demonstrated the role of PAF and its receptor in mediating tissue injury, shock and lethality following endotoxin challenge and other acute inflammatory stimuli (Miotla *et al.*, 1998; Fukuda *et al.*, 2000; Ishii and Shimizu, 2000; Montrucchio *et al.*, 2000; Souza *et al.*, 2000). Thus, during acute bacterial infection,

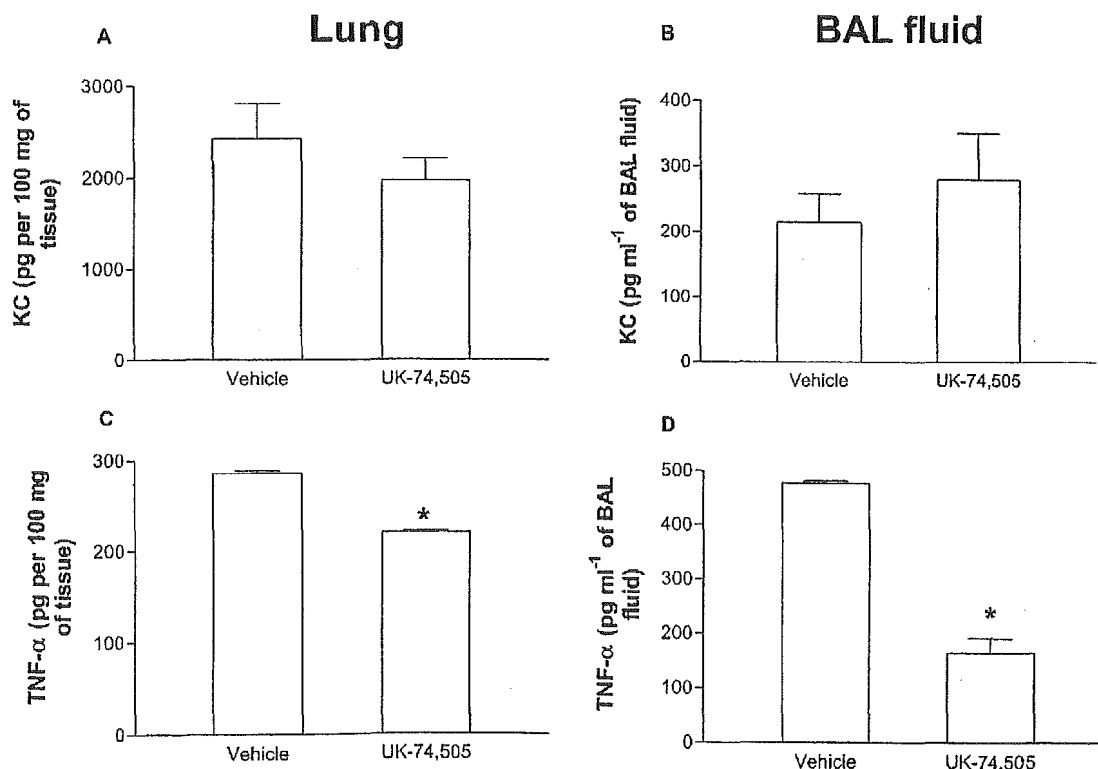


Figure 4 Effect of pre-treatment with the PAF receptor antagonist UK 74,505 on the production of KC and TNF- α after infection with *K. pneumoniae*. Animals were inoculated with 3×10^6 bacteria or vehicle ($30 \mu\text{l}$) and the concentration of KC (A,B) and TNF- α (C,D) in lung tissue (A,C) or BAL fluid (B,D) evaluated by ELISA after 24 h. Results are shown as the mean \pm s.e. mean of six animals in each group. * $P < 0.01$ when compared with animals treated with vehicle.

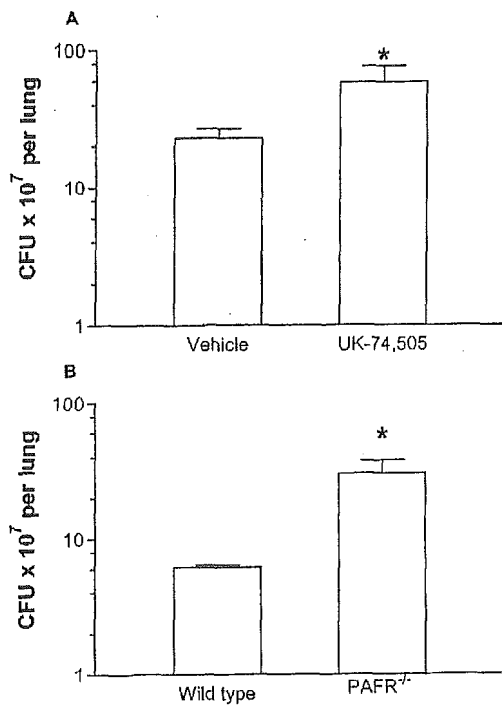


Figure 5 Number of colony-forming units (CFU) after infection with *K. pneumoniae* (A) after the pre-treatment with the PAF receptor antagonist UK 74,505 or in (B) PAFR^{-/-} mice. Animals were inoculated with 3×10^6 bacteria or vehicle (30 μ l) and the number of CFU in lung homogenates evaluated after 24 h. PAFR^{-/-} mice were compared to their respective wild-type controls. Results are shown as the mean \pm s.e. mean of five animals in each group. * $P < 0.01$ when compared with animals treated with vehicle-treated wild-type controls.

Table 1 Percentage of neutrophils from bronchoalveolar lavage of *K. pneumoniae* infected mice containing at least one bacterium in the cytoplasm

| Groups | % neutrophils containing bacteria |
|------------------------------|-----------------------------------|
| Wild type or vehicle treated | 62.2 \pm 3.3 |
| UK-74,505 treated | 31.1 \pm 6.3* |
| PAFR ^{-/-} | 10.1 \pm 5.1* |

Animals were inoculated with 3×10^6 bacteria or vehicle (30 μ l) and the percentage of neutrophils containing at least one bacterium in the cytoplasm was assessed. Results are shown as the mean \pm s.e. mean of 3–6 animals in each group. * $P < 0.01$ when compared with animals treated with vehicle-treated wild-type controls.

activation of PAFR may be important for the ability of the host to deal with infection but could underlie or contribute to the systemic inflammatory response observed in the most severe cases. These possible dual effects of PAFR activation led us to investigate the functional role of the receptor in a model of lung infection with *K. pneumoniae*.

In our model of lung infection, we chose to use *K. pneumoniae* for several reasons. This gram-negative aerobic organism is an important cause of community-acquired pneumonia in individuals with impaired pulmonary defences and is a major pathogen for nosocomial pneumonia (Granton & Grossman, 1993; Maloney & Jarvi, 1995). Importantly, preliminary studies showed that after intratracheal (i.t.)

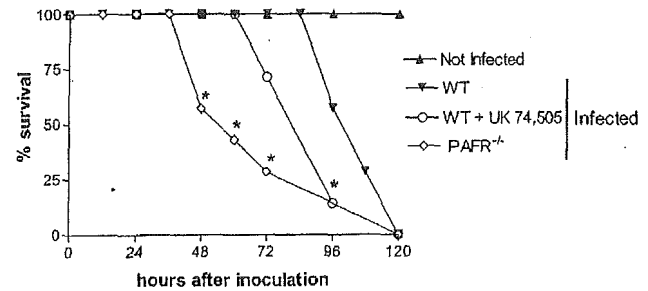


Figure 6 Role of the PAF receptor for the survival of animals after infection with *K. pneumoniae*. Four groups of animals were evaluated (eight animals in each group): infected animals (inoculated with 3×10^6 bacteria) which were PAF receptor-deficient (PAFR^{-/-}), wild-type (Infected WT) or wild-type treated with the PAF receptor antagonist UK 74,505 (WT + UK 74,505) and animals which received only vehicle (30 μ l, not infected). The number of dead animals was evaluated every 12 h and results are shown as per cent survival. Survival of PAFR^{-/-} and UK 74,505-treated animals was significantly different from that of infected WT animals ($P < 0.05$).

inoculation with *K. pneumoniae* mice developed pneumonia with features resembling human disease. Moreover, there is a reproducible relationship between the size of the inoculum and lethality of infection (Toews *et al.*, 1979). A dose of 3×10^6 bacteria was chosen for all experiments as this dose allowed for the development of substantial inflammation within 24 to 48 h without excessive mortality. Untreated animals receiving this dose of *K. pneumoniae* were unable to clear the bacteria and all animals ultimately died. Therefore, this dose allowed for assessment of the inflammatory mediators and bacterial growth, as well as the effects on survival.

In our experiments, the inoculation of *K. pneumoniae* induced a time-dependent increase of infiltration of neutrophils and pro-inflammatory cytokines in the lungs of infected mice. The number of neutrophils increased rapidly and was markedly elevated 24 h after the infection. The increase in neutrophil numbers in BAL fluid and lungs was preceded by an increase in the concentrations of TNF- α and KC. Of note, these pro-inflammatory mediators have been shown to play important roles in the control of bacterial infection and lung inflammation following pulmonary infection with *K. pneumoniae* (Laichalk *et al.*, 1996; Tsai *et al.*, 1998; 2000). Interestingly, at the inoculum used and at time points observed, the inflammatory response seemed to be mostly compartmentalized in the lungs, as the number of leukocytes, and the concentration of cytokines (with the exception of KC) and bacteria were not significantly elevated in the plasma of infected animals. Only later was the control of the infection lost and lethality occurred. Overall, our experiments are in good agreement with observations of other studies examining pulmonary inflammation after *K. pneumoniae* infection (e.g.: Laichalk *et al.*, 1996; Tsai *et al.*, 1998; 2000).

Daily treatment with the PAFR antagonist UK-74,505 had no relevant effect on the influx of neutrophils, as assessed by the number of these cells in BAL fluid, MPO activity and histological analysis of lung tissue. Previous studies have suggested a role for neutrophil-active (CXC) chemokines and chemokine receptors for the migration of neutrophils into the lungs of mice infected with bacteria (Greenberger *et al.*, 1996; Moore *et al.*, 2000; Tsai *et al.*, 2000; Fillion *et al.*, 2001). In addition to the lack of effect of PAFR blockade on neutrophil influx, UK-74,505 had little effect on the tissue

concentrations of the CXC chemokine KC. These results suggest that the early generation of PAF does not play a role in the generation of the neutrophil-active chemokine KC and subsequent sequestration of neutrophils into the lungs of infected mice. Similarly, PAF failed to affect the recruitment of neutrophils to the lungs after *i.v.* challenge with endotoxin (Miotla *et al.*, 1998) or after acid-induced lung injury (Nagase *et al.*, 1999) in mice. Thus, whereas PAFR activation may play a role in phagocytosis-dependent production of the CXC chemokine IL-8 after stimulation with a particulate stimulus (zymosan) (Au *et al.*, 2001), production of KC after bacterial infection *in vivo* seemed to be independent of PAFR activation.

Previous studies (Laichalk *et al.*, 1996) have shown a critical role of TNF- α as part of the pulmonary host defense in a murine model of infection with *K. pneumoniae*. In our model, there was a marked pulmonary production of TNF- α that peaked early after infection and was maximal around 24 h. Pretreatment with UK-74,505 significantly reduced the concentrations of TNF- α both in BAL fluid and pulmonary tissue extracts after *K. pneumoniae* infection. These effects of PAF on TNF- α production seemed to be of physiopathological relevance, as demonstrated by the increase in the number of CFU in the lungs of *K. pneumoniae*-infected mice. The increase in bacterial counts in the lungs were reflected in the severity of the disease, as UK-74,505-treated animals died significantly faster than vehicle-treated controls. Our lethality results are in contrast with a previously published study evaluating the effect of a distinct, shorter-acting PAFR antagonist (WEB2170) in a model of *K. pneumoniae* infection in NMRI mice (Makristathis *et al.*, 1993). In this latter study, WEB2170 treatment was accompanied by a small, dose-independent increase in survival and a marginal, dose-independent decrease in bacterial counts. Moreover, statistical analysis was not provided in that study (Makristathis *et al.*, 1993).

The role of PAFR for the ability of the host to mount an effective immune response was even more markedly appreciated when PAFR-deficient animals were used. In these animals, significant lethality was already noticeable 48 h after infection. Thus, our results clearly suggest that the ability of PAFR to modulate TNF- α production in the lungs of mice may be relevant for an effective innate immune response against *K. pneumoniae* pulmonary infection.

An important role for PAFR in the phagocytosis of particulate stimuli and ensuing pro-inflammatory cytokine production has been demonstrated in several studies (Au *et al.*, 1994, 2001; Aliberti *et al.*, 1999; Owaki *et al.*, 2000). Interestingly, the phagocytosis of *K. pneumoniae* by neutro-

phils is accompanied by the release of PAF from neutrophils (Makristathis *et al.*, 1993). One possibility that stems from the latter observations is that, in our model, the blockade of PAFR may have prevented the ability of phagocytes to engulf bacteria and produce pro-inflammatory cytokines, such as TNF- α , in response to the phagocytic stimulus. In this regard, results of the pre-treatment with UK-74,505 or experiments with PAFR^{-/-} mice showed that fewer neutrophils that migrated to the lungs after *K. pneumoniae* infection ingested bacteria. Moreover, a role of intracellular PAF for the production of TNF- α by macrophages has been previously demonstrated *in vitro* (Yamada *et al.*, 1999; Tsuyuki *et al.*, 2002). Overall, the results above argue for an important role of PAFR activation in mediating the phagocytosis of bacteria. The latter possibility is being actively investigated in our laboratory.

The CC chemokine MCP-1 appears to play an important role in the pulmonary anti-fungal response after *Aspergillus fumigatus* and *Cryptococcus neoformans* infection in mice (Huffnagel *et al.*, 1995; Blease *et al.*, 2001). Similarly, administration of MCP-1 prior to a systemic infection with *Pseudomonas aeruginosa* enhanced survival, an effect associated with enhanced bacterial phagocytosis and killing *in vitro* (Nakano *et al.*, 1994). Nevertheless, several studies have now shown that MCP-1 may shift the balance in favour of anti-inflammatory cytokine production after endotoxin challenge or during septic peritonitis (Matsukawa *et al.*, 2000; Zisman *et al.*, 1997; Hogaboam *et al.*, 1998). There was a marked increase in pulmonary MCP-1 concentrations 24 h after infection with *K. pneumoniae*. Pretreatment with UK-74,505 failed to affect MCP-1 concentrations significantly in our system, excluding a role for PAFR in modulating MCP-1 production.

In conclusion, our results suggest that PAF, by acting on its receptor, plays little role in the local production of chemokines and recruitment of leukocytes during *K. pneumoniae* infection in mice. However, the PAFR appears to contribute to the local production of TNF- α and to the ability of leukocytes to deal with the infecting bacteria. The latter roles of the PAFR may underlie the increased lethality observed in animals treated with a PAFR antagonist or in PAFR^{-/-} mice. Thus, whereas PAFR antagonism appears to be an effective strategy to control the lung injury associated with a range of acute inflammatory stimuli, this receptor is also part of an effective innate immune response against bacterial infection in the lungs. The latter effects of PAFR antagonists may be relevant in humans and could limit any beneficial effects of the drugs in acute inflammatory conditions, such as sepsis.

References

- ALABASTER, V.A., KEIR, R.F., PARRY, M.J. & DE SOUZA, R.N. (1991). UK-74,505, a novel and selective PAF antagonist, exhibits potent and long lasting activity *in vivo*. *Agents Actions Suppl.* **34**, 221–227.
- ALIBERTI, J.C.S., MACHADO, F.S., GAZZINELLI, R.T., TEIXEIRA, M.M. & SILVA, J.S. (1999). Platelet-activating factor induces nitric oxide synthesis in *Trypanosoma cruzi*-infected macrophages and mediates resistance to parasite infection in mice. *Infect. Immun.*, **67**, 2810–2814.
- AU, B.T., TEIXEIRA, M.M., COLLINS, P.D. & WILLIAMS, T.J. (2001). Blockade of PAF receptors controls interleukin-8 production by regulating the activation of neutrophil CD11/CD18. *Eur. J. Pharmacol.*, **425**, 65–71.
- AU, B.T., WILLIAMS, T.J. & COLLINS, P.D. (1994). Zymosan-induced IL-8 release from human neutrophils involves activation via the CD11b/CD18 receptor and endogenous platelet-activating factor as an autocrine modulator. *J. Immunol.*, **152**, 5411–5419.

Reprinted from

PROSTAGLANDINS & other Lipid Mediators

An International Journal

Prostaglandins & other Lipid Mediators 68–69 (2002) 599–609

Platelet-activating factor receptor

Satoshi Ishii^{a,c,*}, Takahide Nagase^b, Takao Shimizu^{a,c}

^a *Department of Biochemistry and Molecular Biology, Faculty of Medicine, The University of Tokyo,
7-3-1 Hongo, Bunkyo-ku, Tokyo 113-0033, Japan*

^b *Department of Geriatric Medicine, Faculty of Medicine, The University of Tokyo, 7-3-1 Hongo,
Bunkyo-ku, Tokyo 113-0033, Japan*

^c *CREST of Japan Science and Technology Corporation, 7-3-1 Hongo, Bunkyo-ku, Tokyo 113-0033, Japan*



ELSEVIER



ELSEVIER

Prostaglandins & other Lipid Mediators 68–69 (2002) 599–609

**PROSTAGLANDINS
& other
LIPID MEDIATORS**

Platelet-activating factor receptor

Satoshi Ishii^{a,c,*}, Takahide Nagase^b, Takao Shimizu^{a,c}^a *Department of Biochemistry and Molecular Biology, Faculty of Medicine, The University of Tokyo, 7-3-1 Hongo, Bunkyo-ku, Tokyo 113-0033, Japan*^b *Department of Geriatric Medicine, Faculty of Medicine, The University of Tokyo, 7-3-1 Hongo, Bunkyo-ku, Tokyo 113-0033, Japan*^c *CREST of Japan Science and Technology Corporation, 7-3-1 Hongo, Bunkyo-ku, Tokyo 113-0033, Japan*

Abstract

Platelet-activating factor (PAF, 1-*O*-alkyl-2-acetyl-*sn*-glycero-3-phosphocholine) is a biologically active phospholipid mediator. Although PAF was named for its potential to induce platelet aggregation, intense investigations have elucidated potent biological actions of PAF in a broad range of cell types and tissues. PAF acts by binding to a unique G-protein-coupled seven transmembrane receptor, and activates multiple intracellular signaling pathways. In the last decade, we have identified the PAF receptor structures, intracellular signaling mechanisms, and genomic organizations. Recently, we found a single nucleotide polymorphism of the human PAF receptor (A224D) with an allele frequency of 7.8% in Japanese. Cells expressing this receptor exhibited the reduced cellular signaling, although the binding parameters remain unchanged. We have established two different types of genetically altered mice, i.e. PAF receptor-overexpressing mouse and PAF receptor-deficient mouse. These mutant mice provide a novel and specific approach for identifying the pathophysiological and physiological functions of PAF *in vivo*. This review focuses on phenotypes of these mutant mice and summarizes the previous reports regarding PAF and PAF receptor.

© 2002 Elsevier Science Inc. All rights reserved.

Keywords: Platelet-activating factor; Phospholipid mediator; Intracellular signaling pathways

1. Introduction

Phospholipids are major components of cellular membranes. They are also known to be sources of arachidonic acid, which is metabolized into bioactive eicosanoids. Some

Abbreviations: PAF, platelet-activating factor; FISH, fluorescence in situ hybridization; PAFR-Tg, PAF receptor transgenic; PAFR-KO, PAF receptor-deficient; WT, wild-type; Mch, methacholine; TX, thromboxane; LT, leukotriene; BrdU, 5-bromo-2'-deoxyuridine

* Corresponding author. Tel.: +81-3-5802-2925; fax: +81-3-3813-8732.

E-mail address: mame@m.u-tokyo.ac.jp (S. Ishii).

0090-6980/02/\$ – see front matter © 2002 Elsevier Science Inc. All rights reserved.

PII: S0090-6980(02)00058-8

3.1. Establishment of PAF receptor mutant mice

PAFR-Tg mice were created by injecting a transgene containing guinea-pig PAF receptor cDNA into the pronuclei of fertilized eggs from BDF1 female mice [47]. The genetic background of the mice used in the experiments was mostly a random mixture of C57BL/6 and DBA/2 alleles. The guinea-pig PAF receptor cDNA was placed under the regulation of cytomegalovirus-immediate early enhancer and β -actin promoter for ubiquitous expression in mice. However, Northern analysis revealed a varied pattern of transgene expression in the established transgenic mouse line: high levels of expression were seen in heart and skeletal muscle, medium levels in eye, skin, trachea and aorta, and barely detectable levels in neutrophils, brain, lung, liver, spleen, kidney, small intestine, uterus and testis. This may suggest that ubiquitous overexpression of PAF receptor was lethal to mouse embryos, so that the PAFR-Tg line that expressed PAF receptor in the pattern described above might have been naturally selected. Expression of the PAF receptor transgene in the early embryonic stage can be deduced from other studies using the same expression unit [48–50].

PAFR-KO mice were created by targeted gene disruption of the PAF receptor gene in E14-1 embryonic stem cells derived from 129/Ola mouse [51]. Unless otherwise stated, the genetic background of PAFR-KO mice is mostly a random mixture of 129/Ola and C57BL/6 alleles. Inactivation of the PAF receptor gene was confirmed by genomic Southern analysis and by Northern analysis of RNA isolated from neutrophils. Neither peritoneal macrophages nor lung tissues from PAFR-KO mice displayed any detectable binding sites for a PAF antagonist WEB 2086, which confirms the loss of surface receptors from these tissues. In PAFR-KO mice, a challenge with PAF no longer induced an increase in intracellular calcium concentrations in casein-elicited peritoneal exudate cells [51], a decrease in arterial pressure [51], a chemotactic response of microglia [52], or arrhythmogenic responses of ventricular myocytes [53]. These results provide compelling evidence that the targeted PAF receptor plays a crucial role in the PAF bioactions. No gross morphological abnormalities were detected in PAFR-KO mice.

3.2. Phenotypes of PAF receptor mutant mice

3.2.1. Reproduction

When heterozygous transgenic males were mated to wild-type (WT) females, the proportion of PAFR-Tg progeny to WT progeny (1:2.3) was significantly lower than that which would be expected from a Mendelian distribution (1:1) [47]. Despite the restricted pattern of transgene expression, a fraction of PAFR-Tg embryos still may not survive gestation. Heterozygous female PAFR-Tg mice produced fewer transgenic progenies, suggesting that a higher expression of PAF receptor in the maternal reproductive system easily causes disorders in fertilization. Interestingly, PAFR-KO mice possessed apparently normal reproductive potential [51]. Taken together, PAF is unlikely to be essential for murine reproduction *in vivo*, but spatiotemporally aberrant expression of the PAF receptor appears to prevent normal ontogeny by collapsing the regulated PAF receptor expression pattern in embryo and uterus. On the other hand, sperm from PAFR-KO mice, which have been backcrossed to C57BL/6 mice more than 10 times, gave a significantly lower rate of *in vitro* fertilization

(21.5%) than did WT sperm (66.7%) [54]. This report suggests that PAF potentiates the capacity of sperm for in vivo fertilization.

3.2.2. Bronchial hyperresponsiveness

Although there were no inflammatory symptoms in the airways of PAFR-Tg mice under physiological conditions, they showed congenital bronchial hyperresponsiveness to inhaled PAF and Mch, a muscarinic receptor agonist [47,55,56]. Because no significant hyperresponsiveness to serotonin was observed in PAFR-Tg mice [56], PAF receptor-overexpression is unlikely to affect general bronchial responsiveness. In response to PAF, the lung resistance in PAFR-Tg mice was increased by several folds largely due to bronchoconstriction, while the airways of WT mice were refractory to PAF [47]. The PAF-induced increase in lung resistance was greatly attenuated not only by the PAF antagonist WEB 2086, but also by a cyclooxygenase inhibitor indomethacin, a thromboxane (TX) synthase inhibitor ozagrel, a 5-lipoxygenase-activating protein inhibitor MK-886, and a cysteinyl leukotriene (LT) antagonist pranlukast [55]. An LTB₄ antagonist ONO-4057, however, had no effects. Therefore, TXA₂ and cysteinyl LTs, which are possibly released in response to PAF, may enhance the PAF-elicited airway response [57,58]. Since the inhibitory effect of each drug was fairly large, the direct role of PAF in bronchoconstriction seems to be much smaller than that of TXA₂ and cysteinyl LTs. Moreover, inhibition of TX synthesis seems to reduce the potent actions of cysteinyl LTs and vice versa. Probably, TXA₂ and cysteinyl LTs exert contractile effects synergistically on the airways of PAFR-Tg mice.

Pretreatment of PAFR-Tg mice with a PAF antagonist, a TX synthase inhibitor, or a cysteinyl LT antagonist significantly reduced the hyperresponsiveness to Mch, one of the major manifestations of asthma [47,55]. These results suggest that there is an interrelation between Mch and PAF hyperresponsiveness as well as a contribution of PAF to the etiology of asthma. However, the binding assays for muscarinic receptors revealed no difference in K_d or B_{max} value between PAFR-Tg and WT mice [56]. Thus, a potential mechanism underlying hyperresponsiveness to Mch is that Mch-stimulated release of PAF may lead to overproduction of TXA₂ and cysteinyl LTs in PAFR-Tg mice. Unexpectedly, Mch appears to mediate the bronchoconstrictive action of PAF in PAFR-Tg mice, since atropine, an antagonist for muscarinic receptors, strongly blocked the PAF-induced airway responses [56]. This report suggests that a synergistic effect between PAF and Mch also exists in the airways of PAFR-Tg mice.

3.2.3. Systemic anaphylaxis

Actively sensitized PAFR-KO mice showed drastically attenuated systemic anaphylactic responses—hypotension, heart rate change, lung resistance elevation with bronchoconstriction, and lung edema—after antigen challenge [51]. PAFR-KO mice were also more likely to survive systemic anaphylaxis compared with WT mice. These results demonstrate a dominant role of PAF in murine anaphylaxis, although there are various other anaphylactic mediators, such as eicosanoids, histamine, and serotonin.

3.2.4. Inflammation

When hydrochloric acid (HCl) was given intratracheally, PAFR-Tg mice showed more severe lung injury—increases in lung elastance, development of pulmonary edema, and

deterioration of gas exchange—compared to WT mice [59]. The symptoms of PAFR-KO mice were significantly milder than those of WT mice. But, the degree of neutrophil sequestration in the lung was similar in both mutant mice. These observations suggest that PAF is involved in the pathogenesis of acute lung injury caused by acid aspiration in mice, except for neutrophil sequestration. For induction of the lung injury, therefore, neutrophil sequestration is not sufficient, but PAF-activation of neutrophils (and/or an as yet unidentified pulmonary cell type) is probably required.

3.2.5. Endotoxic shock

In terms of sensitivity to LPS, phenotypes of PAFR-Tg and PAFR-KO mice were apparently conflicting. The lethality of LPS was significantly higher for PAFR-Tg mice than for WT mice [47]. WEB 2086 afforded good protection against LPS-induced death with PAFR-Tg mice. Contrary to expectations, PAFR-KO mice showed the same sensitivity to LPS as WT mice [51]; two major systemic responses, lethality and hypotension, were normal in PAFR-KO mice. In support of the data, peritoneal macrophages from WT and PAFR-KO mice produced equivalent levels of the two proinflammatory cytokines, IL-1 β and IL-6, in response to LPS. PAF may, therefore, function not as an essential, but as an exaggerating factor for murine endotoxic shock. Since mice are less sensitive to LPS than other experimental animal species [60], the contribution of PAF to endotoxic shock might be congenitally low in mice. This might account for the normal sensitivity to LPS in PAFR-KO mice.

3.2.6. Brain

PAFR-KO mice had no apparent gross malformation in the brain [51], comparable to that seen with *LIS1* gene-disrupted mice [46]. This may suggest that Lis1 protein has other function(s) that are relevant to brain development but unrelated to PAF. PAFR-KO mice exhibited normal LTP and showed no obvious abnormality in excitatory synaptic transmission in the hippocampal CA1 region [61]. However, another group has shown the impairment of LTP in the dentate gyrus in PAFR-KO mice [62]. More detailed studies are needed to draw a definite conclusion with respect to physiological roles for PAF and the PAF receptor in central nervous system.

3.2.7. Skin

Abnormal skin pigmentation was observed in the ear and tail of PAFR-Tg mice, some of which spontaneously progressed into melanocytic tumors [47]. In the skin of the ear and tail, not only melanocytes but also keratinocytes proliferated highly. This hyperplasia increased with aging [63]. Of interest, these skin abnormalities had no effect on the coat color of PAFR-Tg mice, indicating a normal functioning of melanocytes in hair follicles. In an experiment using *in situ* hybridization, expression of the transgene (guinea-pig PAF receptor cDNA) was observed in keratinocytes but not in melanocytes [63]. Furthermore, the melanocytic tumors only weakly expressed guinea-pig PAF receptor mRNA and proteins (unpublished data). These results suggest that the hyperplasia of melanocytes is due to an indirect effect of PAF receptor overexpression. Since keratinocytes are known to produce growth factors for melanocytes, including basic fibroblast growth factor [64], endothelin-1 [65], and stem cell factor [66], PAF receptor-overexpression in keratinocytes

may result in abnormal production of various growth factors that can cause hyperplasia of melanocytes.

Accelerated proliferation of keratinocytes in PAFR-Tg mice was demonstrated by incorporation of 5-bromo-2'-deoxyuridine (BrdU) in vivo [63]. Treatment with a WEB 2086 ointment reduced the number of BrdU-positive cells. Hence, these results confirm the potential of PAF receptor-overexpression to proliferate keratinocytes in vivo. Interestingly, a decrease in BrdU-positive cells was also observed in WT mice, suggesting that PAF is involved in keratinocyte proliferation under physiological conditions.

PAFR-KO mice show no spontaneous abnormalities in the skin. Thus, PAF does not appear to be essential for the skin in terms of morphogenesis and proliferation under normal physiological conditions. It is noteworthy, however, that aberrant expression of the PAF receptor has the potential to elicit skin diseases.

3.2.8. PAF metabolism

As for low-density lipoprotein and thrombopoietin, their cognate receptors are reported to regulate the ligand concentration in the extracellular space [67,68]. Receptor-dependent metabolism of the ligands is likely to be responsible for the phenomenon. Thus, PAFR-KO mice, which have been backcrossed to C57BL/6 mice six to seven times, were used to examine the receptor-dependent metabolism, i.e. production and degradation of PAF. In casein-elicited peritoneal exudate cells rich in neutrophils, a calcium ionophore A23187 enhances PAF production [69]. PAF receptor deficiency, however, did not cause a change of either the basal PAF level or the PAF-producing ability of these cells. On the other hand, thioglycollate-elicited peritoneal macrophages from PAFR-KO mice exhibit half the capacity for PAF-degradation of WT mice [70]. The reduction was ascribed to the deficiencies of receptor-dependent PAF uptake and PAF acetylhydrolase release in PAFR-KO mice.

4. Closing remarks

This review has provided an update of our knowledge of PAF and the PAF receptor, focusing on the human PAF receptor mutant and the phenotypes of genetically altered mice.

In investigating the function of the PAF receptor, the overwhelming advantage of the transgenic approach over the conventional pharmacological one is the complete selectivity obtained in PAFR-Tg and PAFR-KO mice. Indeed, several PAF antagonists were demonstrated to have dual activities blocking PAF receptor-mediated activation but also inhibiting other enzymes, including cyclooxygenase [71], lipoxygenase [71], phospholipase A2 [72], acetylcholinesterase [73], and intracellular PAF acetylhydrolase [74,75]. Some other PAF antagonists inhibited histamine effects through interaction with the histamine G-protein-coupled receptor [76–78]. The disadvantage of the transgenic approach is the limitation of species; we are allowed to utilize only mouse, particularly in the case of a gene-targeted animal. Since much research on PAF has dealt with other species besides the mouse, e.g. human, dog, rat, and guinea-pig, it is conceivable that species-specific phenomena may cause confusion in interpreting the data. Historically, the use of new strategies and the interpretation of data derived from them become more sophisticated with time.

Although we recognize that PAF receptor mutant mice are not a panacea for PAF research, they should contribute greatly to our understanding of the physiological and pathophysiological functions of PAF, along with pharmacological and genetic approaches.

Acknowledgements

We thank collaborators who obtained the findings we have reviewed in this article.

References

- [1] Benveniste J, Henson PM, Cochrane CG. Leukocyte-dependent histamine release from rabbit platelets: the role of IgE, basophils and a platelet-activating factor. *J Exp Med* 1972;136:1356.
- [2] Demopoulos CA, Pinckard RN, Hanahan DJ. Platelet-activating factor. Evidence for 1-*O*-alkyl-2-acetyl-*sn*-glyceryl-3-phosphorylcholine as the active component (a new class of lipid chemical mediators). *J Biol Chem* 1979;254:9355.
- [3] Blank ML, Snyder F, Byers LW, Brooks B, Muirhead EE. Antihypertensive activity of an alkyl ether analog of phosphatidylcholine. *Biochem Biophys Res Commun* 1979;90:1194.
- [4] Benveniste J, Tence M, Varenne P, Bidault J, Bouillet C, Polonsky J. Semi-synthesis and proposed structure of platelet-activating factor (PAF): PAF-acether an alkyl ether analog of lysophosphatidylcholine. *C R Acad Sci D* 1979;289:1037.
- [5] Hanahan DJ. Platelet activating factor: a biologically active phosphoglyceride. *Annu Rev Biochem* 1986;55:483.
- [6] Chao W, Olson MS. Platelet-activating factor: receptors and signal transduction. *Biochem J* 1993;292:617.
- [7] Snyder F. The ether lipid trail: a historical perspective. *Biochim Biophys Acta* 1999;1436:265.
- [8] Shimizu T, Honda Z, Nakamura M, Bito H, Izumi T. Platelet-activating factor receptor and signal transduction. *Biochem Pharmacol* 1992;44:1001.
- [9] Izumi T, Shimizu T. Platelet-activating factor receptor: gene expression and signal transduction. *Biochim Biophys Acta* 1995;1259:317.
- [10] Ishii S, Shimizu T. Platelet-activating factor (PAF) receptor and genetically engineered PAF receptor mutant mice. *Prog Lipid Res* 2000;39:41.
- [11] Prescott SM, Zimmerman GA, Stafforini DM, McIntyre TM. Platelet-activating factor and related lipid mediators. *Annu Rev Biochem* 2000;69:419.
- [12] Snyder F. Platelet-activating factor and its analogs: metabolic pathways and related intracellular processes. *Biochim Biophys Acta* 1995;1254:231.
- [13] Snyder F. Platelet-activating factor: the biosynthetic and catabolic enzymes. *Biochem J* 1995;305:689.
- [14] Honda Z, Nakamura M, Miki I, Minami M, Watanabe T, Seyama Y, et al. Cloning by functional expression of platelet-activating factor receptor from guinea-pig lung. *Nature* 1991;349:342.
- [15] Bito H, Honda Z, Nakamura M, Shimizu T. Cloning, expression and tissue distribution of rat platelet-activating-factor-receptor cDNA. *Eur J Biochem* 1994;221:211.
- [16] Nakamura M, Honda Z, Izumi T, Sakanaka C, Mutoh H, Minami M, et al. Molecular cloning and expression of platelet-activating factor receptor from human leukocytes. *J Biol Chem* 1991;266:20400.
- [17] Kunz D, Gerard NP, Gerard C. The human leukocyte platelet-activating factor receptor: cDNA cloning, cell surface expression, and construction of a novel epitope-bearing analog. *J Biol Chem* 1992;267:9101.
- [18] Ye RD, Prossnitz ER, Zou AH, Cochrane CG. Characterization of a human cDNA that encodes a functional receptor for platelet activating factor. *Biochem Biophys Res Commun* 1991;180:105.
- [19] Sugimoto T, Tsuchimochi H, McGregor CG, Mutoh H, Shimizu T, Kurachi Y. Molecular cloning and characterization of the platelet-activating factor receptor gene expressed in the human heart. *Biochem Biophys Res Commun* 1992;189:617.
- [20] Izumi T, Kishimoto S, Takano T, Nakamura M, Miyabe Y, Nakata M, et al. Expression of human platelet-activating factor receptor gene in EoL-1 cells following butyrate-induced differentiation. *Biochem J* 1995;305:829.

- [21] Mutoh H, Bito H, Minami M, Nakamura M, Honda Z, Izumi T, et al. Two different promoters direct expression of two distinct forms of mRNAs of human platelet-activating factor receptor. *FEBS Lett* 1993;322:129.
- [22] Seyfried CE, Schweickart VL, Godiska R, Gray PW. The human platelet-activating factor receptor gene (PTAFR) contains no introns and maps to chromosome 1. *Genomics* 1992;13:832.
- [23] Chase PB, Halonen M, Regan JW. Cloning of a human platelet-activating factor receptor gene: evidence for an intron in the 5'-untranslated region. *Am J Respir Cell Mol Biol* 1993;8:240.
- [24] Ishii S, Matsuda Y, Nakamura M, Waga I, Kume K, Izumi T, et al. A murine platelet-activating factor receptor gene: cloning, chromosomal localization and up-regulation of expression by lipopolysaccharide in peritoneal resident macrophages. *Biochem J* 1996;314:671.
- [25] Chase PB, Yang JM, Thompson FH, Halonen M, Regan JW. Regional mapping of the human platelet-activating factor receptor gene (PTAFR) to 1p35 → p34.3 by fluorescence in situ hybridization. *Cytogenet Cell Genet* 1996;72:205.
- [26] Abbott CA, Blank R, Eppig JT, Fiedorek Jr FT, Frankel W, Friedman JM, et al. Mouse chromosome 4. *Mammal Genome* 1994;5:S51.
- [27] Chen J, Giri SN. Differences in platelet-activating factor receptor mediated Ca^{2+} response between hamster and guinea pig alveolar macrophages. *J Pharmacol Exp Ther* 1997;281:1047.
- [28] Centemeri C, Colli S, Tosarello D, Ciceri P, Nicosia S. Heterogeneous platelet-activating factor (PAF) receptors and calcium increase in platelets and macrophages. *Biochem Pharmacol* 1999;57:263.
- [29] Fukunaga K, Ishii S, Asano K, Yokomizo T, Shiomi T, Shimizu T, et al. Single nucleotide polymorphism of human platelet-activating factor receptor impairs G-protein activation. *J Biol Chem* 2001;276:43025.
- [30] Hanahan DJ, Demopoulos CA, Liehr J, Pinckard RN. Identification of platelet activating factor isolated from rabbit basophils as acetyl glyceryl ether phosphocholine. *J Biol Chem* 1980;255:5514.
- [31] Mencia-Huerta JM, Lewis RA, Razin E, Austen KF. Antigen-initiated release of platelet-activating factor (PAF-acether) from mouse bone marrow-derived mast cells sensitized with monoclonal IgE. *J Immunol* 1983;131:2958.
- [32] Ikegami K, Hata H, Fuchigami J, Tanaka K, Kohjimoto Y, Uchida S, et al, Tasaka K. Apafant (a PAF receptor antagonist) suppresses the early and late airway responses in guinea pigs: a comparison with antiasthmatic drugs. *Eur J Pharmacol* 1997;328:75.
- [33] Miwa M, Miyake T, Yamanaka T, Sugatani J, Suzuki Y, Sakata S, et al. Characterization of serum platelet-activating factor (PAF) acetylhydrolase: correlation between deficiency of serum PAF acetylhydrolase and respiratory symptoms in asthmatic children. *J Clin Invest* 1988;82:1983.
- [34] Stafforini DM, Satoh K, Atkinson DL, Tjoelker LW, Eberhardt C, Yoshida H, et al. Platelet-activating factor acetylhydrolase deficiency: a missense mutation near the active site of an anti-inflammatory phospholipase. *J Clin Invest* 1996;97:2784.
- [35] Stafforini DM, McIntyre TM, Zimmerman GA, Prescott SM. Platelet-activating factor acetylhydrolases. *J Biol Chem* 1997;272:17895.
- [36] Stafforini DM, Numao T, Tsodikov A, Vaitkus D, Fukuda T, Watanabe N, et al. Deficiency of platelet-activating factor acetylhydrolase is a severity factor for asthma. *J Clin Invest* 1999;103:989.
- [37] Tsukioka K, Matsuzaki M, Nakamata M, Kayahara H, Nakagawa T. Increased plasma level of platelet-activating factor (PAF) and decreased serum PAF acetylhydrolase (PAFAH) activity in adults with bronchial asthma. *J Invest Allergol Clin Immunol* 1996;6:22.
- [38] Albert DH, Magoc TJ, Tapang P, Luo G, Morgan DW, Curtin M, et al. Pharmacology of ABT-491, a highly potent platelet-activating factor receptor antagonist. *Eur J Pharmacol* 1997;325:69.
- [39] Qu XW, Rozenfeld RA, Huang W, Crawford SE, Gonzalez CF, Hsueh W. Interaction of platelet-activating factor, spleen and atrial natriuretic peptide in plasma volume regulation during endotoxaemia in rats. *J Physiol* 1998;512:227.
- [40] Cundell DR, Gerard NP, Gerard C, Idanpaan HI, Tuomanen EI. *Streptococcus pneumoniae* anchor to activated human cells by the receptor for platelet-activating factor. *Nature* 1995;377:435.
- [41] Ring A, Weiser JN, Tuomanen EI. Pneumococcal trafficking across the blood-brain barrier. Molecular analysis of a novel bidirectional pathway. *J Clin Invest* 1998;102:347.
- [42] Izaki S, Yamamoto T, Goto Y, Ishimaru S, Yodate F, Kitamura K, et al. Platelet-activating factor and arachidonic acid metabolites in psoriatic inflammation. *Br J Dermatol* 1996;134:1060.
- [43] Kemeny L, Trach V, Dobozy A. Effect of locally applied WEB 2086, a platelet-activating factor antagonist, on inflammatory skin conditions in mice. *Arch Dermatol Res* 1996;288:492.

- [44] Woodward DF, Nieves AL, Spada CS, Williams LS, Tuckett RP. Characterization of a behavioral model for peripherally evoked itch suggests platelet-activating factor as a potent pruritogen. *J Pharmacol Exp Ther* 1995;272:758.
- [45] Hattori M, Adachi H, Tsujimoto M, Arai H, Inoue K. Miller–Dieker lissencephaly gene encodes a subunit of brain platelet-activating factor acetylhydrolase. *Nature* 1994;370:216.
- [46] Hirotsune S, Fleck MW, Gambello MJ, Bix GJ, Chen A, Clark GD, et al. Graded reduction of Pafah1b1 (Lis1) activity results in neuronal migration defects and early embryonic lethality. *Nat Genet* 1998;19:333.
- [47] Ishii S, Nagase T, Tashiro F, Ikuta K, Sato S, Waga I, et al. Bronchial hyperreactivity, increased endotoxin lethality and melanocytic tumorigenesis in transgenic mice overexpressing platelet-activating factor receptor. *EMBO J* 1997;16:133.
- [48] Araki K, Araki M, Miyazaki J, Vassalli P. Site-specific recombination of a transgene in fertilized eggs by transient expression of Cre recombinase. *Proc Natl Acad Sci USA* 1995;92:160.
- [49] Sunaga S, Maki K, Komagata Y, Ikuta K, Miyazaki JI. Efficient removal of loxP-flanked DNA sequences in a gene-targeted locus by transient expression of Cre recombinase in fertilized eggs. *Mol Reprod Dev* 1997;46:109.
- [50] Sakai K, Miyazaki JI. A transgenic mouse line that retains Cre recombinase activity in mature oocytes irrespective of the cre transgene transmission. *Biochem Biophys Res Commun* 1997;237:318.
- [51] Ishii S, Kuwaki T, Nagase T, Maki K, Tashiro F, Sunaga S, et al. Impaired anaphylactic responses with intact sensitivity to endotoxin in mice lacking a platelet-activating factor receptor. *J Exp Med* 1998;187:1779.
- [52] Aihara M, Ishii S, Kume K, Shimizu T. Interaction between neurone and microglia mediated by platelet-activating factor. *Genes Cells* 2000;5:397.
- [53] Barbuti A, Ishii S, Shimizu T, Robinson RB, Feinmark SJ. Block of the background K⁺ channel, TASK-1, contributes to the arrhythmogenic effects of platelet-activating factor. *Am J Physiol* 2002;282:2024.
- [54] Wu C, Stojanov T, Chami O, Ishii S, Shimizu T, Li A, et al. Evidence for the autocrine induction of capacitation of mammalian spermatozoa. *J Biol Chem* 2001;276:26962.
- [55] Nagase T, Ishii S, Katayama H, Fukuchi Y, Ouchi Y, Shimizu T. Airway responsiveness in transgenic mice overexpressing platelet-activating factor receptor: roles of thromboxanes and leukotrienes. *Am J Respir Crit Care Med* 1997;156:1621.
- [56] Nagase T, Ishii S, Shindou H, Ouchi Y, Shimizu T. Airway hyperresponsiveness in transgenic mice overexpressing platelet activating factor receptor is mediated by an atropine-sensitive pathway. *Am J Respir Crit Care Med* 2002;165:200.
- [57] Wu T, Rieves RD, Logun C, Shelhamer JH. Platelet-activating factor stimulates eicosanoid production in cultured feline tracheal epithelial cells. *Lung* 1995;173:89.
- [58] Gomez FP, Iglesia R, Roca J, Barbera JA, Chung KF, Rodriguez- Roisin R. The effects of 5-lipoxygenase inhibition by zileuton on platelet-activating-factor-induced pulmonary abnormalities in mild asthma. *Am J Respir Crit Care Med* 1998;157:1559.
- [59] Nagase T, Ishii S, Kume K, Uozumi N, Izumi T, Ouchi Y, et al. Platelet-activating factor mediates acid-induced lung injury in genetically-engineered mice. *J Clin Invest* 1999;104:1071.
- [60] Koltai M, Hosford D, Braquet P. PAF-induced amplification of mediator release in septic shock: prevention or downregulation by PAF antagonists. *J Lipid Mediat* 1993;6:183.
- [61] Kobayashi K, Ishii S, Kume K, Takahashi T, Shimizu T, Manabe T. Platelet-activating factor receptor is not required for long-term potentiation in the hippocampal CA1 region. *Eur J Neurosci* 1999;11:1313.
- [62] Chen C, Magee JC, Marcheselli V, Hardy M, Bazan NG. Attenuated LTP in hippocampal dentate gyrus neurons of mice deficient in the PAF receptor. *J Neurophysiol* 2001;85:384.
- [63] Sato S, Kume K, Ito C, Ishii S, Shimizu T. Accelerated proliferation of the epidermal keratinocytes by the transgenic expression of the platelet-activating factor receptor. *Arch Dermatol Res* 1999;291:614.
- [64] Halaban R, Langdon R, Birchall N, Cuono C, Baird A, Scott G, et al. Basic fibroblast growth factor from human keratinocytes is a natural mitogen for melanocytes. *J Cell Biol* 1988;107:1611.
- [65] Imokawa G, Miyagishi M, Yada Y. Endothelin-1 as a new melanogen: coordinated expression of its gene and the tyrosinase gene in UVB-exposed human epidermis. *J Invest Dermatol* 1995;105:32.
- [66] Grabbe J, Welker P, Dippel E, Czarnetzki BM. Stem cell factor, a novel cutaneous growth factor for mast cells and melanocytes. *Arch Dermatol Res* 1994;287:78.
- [67] Ishibashi S, Brown MS, Goldstein JL, Gerard RD, Hammer RE, Herz J. Hypercholesterolemia in low density lipoprotein receptor knockout mice and its reversal by adenovirus-mediated gene delivery. *J Clin Invest* 1993;92:883.

- [68] Gurney AL, Carver-Moore K, de Sauvage FJ, Moore MW. Thrombocytopenia in c-mpl-deficient mice. *Science* 1994;265:1445.
- [69] Shindou H, Ishii S, Uozumi N, Shimizu T. Roles of cytosolic phospholipase A2 and platelet-activating factor receptor in the Ca-induced biosynthesis of PAF. *Biochem Biophys Res Commun* 2000;271:812.
- [70] Ohshima N, Ishii S, Izumi T, Shimizu T. Receptor-dependent metabolism of platelet-activating factor in murine macrophages. *J Biol Chem* 2002;277:9722.
- [71] Saeed SA, Simjee RU, Mahmood F, Rahman NN. Dual inhibition of platelet-activating factor and arachidonic acid metabolism by ajmaline and effect on carrageenan-induced rat paw oedema. *J Pharm Pharmacol* 1993;45:715.
- [72] Hsiao G, Ko FN, Jong TT, Teng CM. Antiplatelet action of 3',4'-diisovalerylhellactone diester purified from *Peucedanum japonicum*. *Thunb Biol Pharm Bull* 1998;21:688.
- [73] Le Texier L, Favre E, Redeuilh C, Blavet N, Bellahsene T, Dive G, et al. Structure-activity relationships in platelet-activating factor (PAF). 7. Tetrahydrofuran derivatives as dual PAF antagonists and acetylcholinesterase inhibitors: synthesis and PAF-antagonistic activity. *J Lipid Mediat Cell Signal* 1996;13:189.
- [74] Svetlov SI, Howard KM, Miwa M, Flickinger BD, Olson MS. Interaction of platelet-activating factor with rat hepatocytes: uptake, translocation, metabolism, and effects on PAF-acetylhydrolase secretion and protein tyrosine phosphorylation. *Arch Biochem Biophys* 1996;327:113.
- [75] Adachi T, Aoki J, Manya H, Asou H, Arai H, Inoue K. PAF analogues capable of inhibiting PAF acetylhydrolase activity suppress migration of isolated rat cerebellar granule cells. *Neurosci Lett* 1997;235:133.
- [76] Piwinski JJ, Wong JK, Green MJ, Ganguly AK, Billah MM, West RJ, et al. Dual antagonists of platelet activating factor and histamine: identification of structural requirements for dual activity of *N*-acyl-4-(5,6-dihydro-11*H*-benzo [5,6]cyclohepta-[1,2-*b*]pyridin-11-ylidene)piperidines. *J Med Chem* 1991;34:457.
- [77] Billah MM, Egan RW, Ganguly AK, Green MJ, Kreutner W, Piwinski JJ, et al. Discovery and preliminary pharmacology of Sch 37370, a dual antagonist of PAF and histamine. *Lipids* 1991;26:1172.
- [78] Merlos M, Giral M, Balsa D, Ferrando R, Queralt M, Puigdemont A, et al. Rupatadine, a new potent, orally active dual antagonist of histamine and platelet-activating factor (PAF). *J Pharmacol Exp Ther* 1997;280:114.

Ginkgolide Derivatives for Photolabeling Studies: Preparation and Pharmacological Evaluation

Kristian Strømgaard,[†] D. Roland Saito,[†] Hideo Shindou,[‡] Satoshi Ishii,[‡] Takao Shimizu,[‡] and Koji Nakanishi*[†]

Department of Chemistry, Columbia University, 3000 Broadway, New York, New York 10027,

Department of Biochemistry and Molecular Biology, Faculty of Medicine, The University of Tokyo, Hongo 7-3-1, Bunkyo-ku, Tokyo 113-0033, Japan, and CREST of Japan Science and Technology Corporation, Tokyo 113-0033, Japan

Received April 4, 2002

The terpene trilactones (TTLs), ginkgolides and bilobalide, are structurally unique constituents of *Ginkgo biloba* extracts, which exhibit various neuromodulatory properties. Although the TTLs are believed to be responsible for some of these effects, the specific interactions with targets in the central nervous system remain to be elucidated on a molecular level. Ginkgolides are known antagonists of the platelet-activating factor (PAF) receptor. Herein, we describe the first examination of the binding of native TTLs and their derivatives to the cloned PAF receptor, confirming that of the TTLs, ginkgolide B is the most potent PAF receptor antagonist. Ginkgolide derivatives carrying photoactivatable and fluorescent groups for the purpose of performing photolabeling have been prepared and evaluated using the cloned PAF receptor. These studies have shown that ginkgolide derivatives with aromatic photoactivatable substituents are potent PAF receptor antagonists with K_i values of 0.09–0.79 μM and hence excellent ligands for clarifying the binding of ginkgolides to PAF receptor by photolabeling studies. Ginkgolide derivatives incorporating both fluorescent and photoactivatable groups still retained binding affinity to the PAF receptor and hence should be promising ligands for photolabeling and subsequent sequencing studies.

Introduction

Ginkgo biloba L., the last surviving member of a family of trees (*Ginkgoaceae*) that appeared more than 250 million years ago, has been mentioned in the Chinese Materia Medica for more than 2500 years.¹ A number of *G. biloba* natural products have been isolated,² the most unique being the terpene trilactones (TTLs), i.e., ginkgolides A, B, C, J, and M (1–5) and bilobalide (6) (Figure 1).^{3–6} The ginkgolides are diterpenes with a cage skeleton consisting of six five-membered rings, i.e., a spiro[4.4]nonane carbocycle, three lactones, and a tetrahydrofuran (THF). The difference between the five ginkgolides lies in the variation in the number and positions of hydroxyl groups on the spirononane framework (Figure 1).

A standardized *G. biloba* extract (EGb 761) containing TTLs (5–7%) and flavonoids (22–24%) has demonstrated neuromodulatory properties,⁷ and several clinical studies using EGb 761 have reported positive effects on various neurodegenerative diseases,^{8–13} including Alzheimer's disease (AD).^{14,15} A recent study by Schultz and co-workers found that EGb 761 upregulated several genes in rat hippocampus and cortex, including genes expressing proteins such as transthyretin and neuronal tyrosine/threonine phosphatase, both of which are believed to be involved in AD.¹⁶ Several recent studies on healthy volunteers have shown positive effects of EGb 761 on short-term working memory indicating that

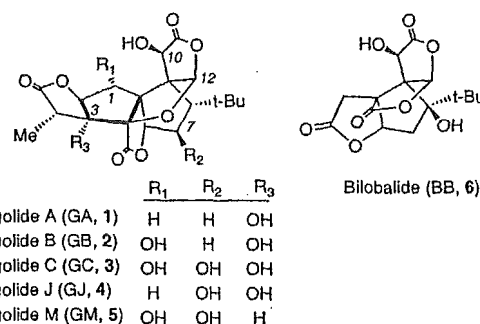


Figure 1. TTLs isolated from *G. biloba*. GA (1), GB (2), and GC (3) are found in the leaves and root bark of *G. biloba*, but GJ (4) is found only in the leaves, and GM (5) is found only in the root bark.

constituents of *G. biloba* also influence the brain under physiological conditions.^{17–20}

Although the molecular basis for the action of *G. biloba* TTL constituents on the central nervous system (CNS) is only poorly understood, it is known that the ginkgolides, particularly ginkgolide B (GB, 2), is a potent *in vitro* antagonist of the platelet-activating factor receptor (PAFR).²¹ PAF (1-*O*-alkyl-2-acetyl-*sn*-glycero-3-phosphocholine, Figure 2) is a phospholipid mediator involved in numerous disorders including acute allergy, inflammation, asthma, and ischemic injury. These effects are manifested through binding of PAF to the PAFR, a G protein-coupled receptor that is found in organs such as the lungs, liver, kidneys,^{22–24} and brain.^{25,26} The function of PAF in the brain is still not clear, although PAF has been suggested to play a role in diseases of aging²⁷ and in initiating human immunodeficiency virus (HIV)-related neuropathogenesis.²⁸ PAF has also been suggested as a retrograde

* To whom correspondence should be addressed. Tel: +1 212 854 2169. Fax: +1 212 932 8273. E-mail: kn5@columbia.edu.

[†] Columbia University.

[‡] The University of Tokyo and CREST of Japan Science and Technology Corp.

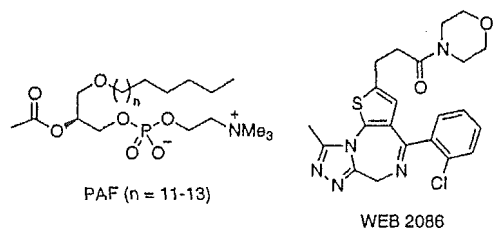


Figure 2. Structures of PAF, the endogenous ligand for the PAFR, and WEB 2086, a potent and selective antagonist, both of which have been used in radioligand binding studies.

messenger in long-term potentiation (LTP).^{29,30} However, studies using PAFR knock-out mice gave contradictory results; one study showed attenuation of LTP in the hippocampal dentate gyrus regions of mice lacking the PAFR,³¹ whereas another study showed that the PAFR was not required for LTP in the hippocampal CA1 region.³² These discrepancies may be due to differences in the hippocampal areas observed, as well as the assay conditions used. However, it is still unclear whether the neuromodulatory effect of TTLs or *G. biloba* extract is related to the PAFR.^{33,34}

With few exceptions, previous structure–activity relationship (SAR) studies of TTLs on the PAFR have focused almost entirely on derivatives of GB (2). In all cases, the derivatives were evaluated for their ability to prevent PAF-induced aggregation of rabbit platelets. Corey et al. investigated various intermediates encountered during the course of the total syntheses of ginkgolide A (GA, 1),³⁵ GB (2),³⁶ and bilobalide (BB, 6)³⁷ and found that although the terminal methyl-bearing lactone was not essential for activity and could be replaced by other lipophilic groups,³⁸ the *tert*-butyl group was important for PAFR antagonism.³⁹ Park et al. synthesized over 200 derivatives of GB (2), with particular focus on aromatic substituents at 10-OH, and found most of them to be more potent than the parent compound.⁴⁰ Similar derivatives recently synthesized by Hu et al. also yielded compounds more potent than GB (2),^{41,42} whereas other variations in GA (1) and GB (2) led to a decrease in activity.^{43,44}

In the following, we describe the first evaluation of the interaction of all native ginkgolides and bilobalide with the cloned PAFR by a radioligand binding assay, as well as their functional properties by intracellular calcium measurements. A series of ginkgolide derivatives with photoactivatable and fluorescent groups have

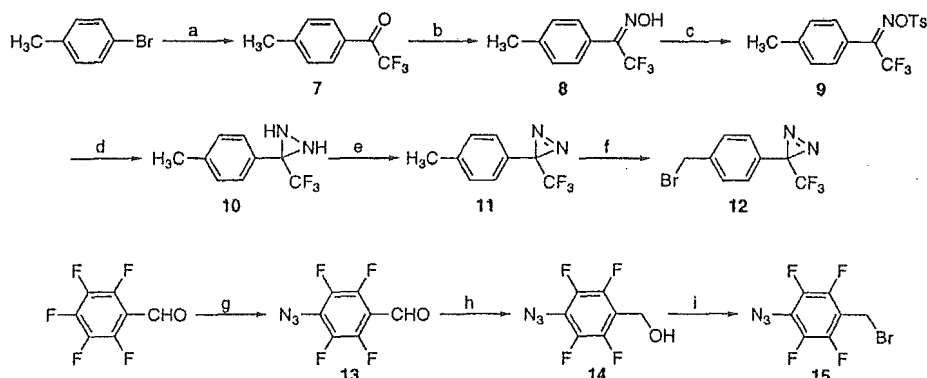
been prepared, and these analogues have been assessed for their ability to displace radioligand binding to cloned PAFR.

Results

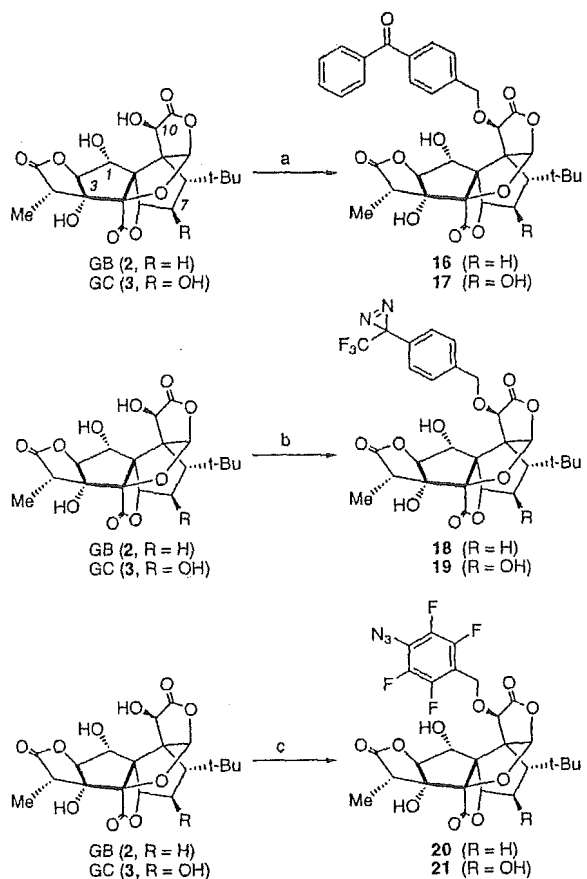
Synthesis. A series of photoactivatable GB (2) and ginkgolide C (GC, 3) derivatives were designed based on previous SAR studies of ginkgolides, which demonstrated that bulky aromatic substituents in the 10-OH position of GB (2) increase activity at the PAFR.^{40–42} Three different photoactivatable moieties, benzophenone, trifluoromethyldiazirine, and tetrafluorophenyl azide, were chosen as they have been described as being among the most successful for labeling receptors and enzymes.^{45–47} Most importantly, upon irradiation, these photoactivatable groups react with the receptor via different intermediates, namely, a radical, a carbene, or a (singlet) nitrene for the benzophenone, trifluoromethyldiazirine, and tetrafluorophenyl azide moieties, respectively.⁴⁵ Because it is essentially impossible to predict which group will be most readily incorporated into the receptor, use of these different groups increases the likelihood of a successful incorporation.

4-(Bromomethyl)benzophenone was commercially available, whereas trifluoromethyldiazirine **12**^{48,49} and tetrafluorophenyl azide **15**^{50–52} were synthesized, respectively, as outlined in Scheme 1. The bromotrifluoromethyldiazirine **12** was synthesized starting from readily available 4-bromotoluene, which was reacted with *N*-trifluoroacetyl piperidine⁴⁸ to give trifluoroacetyl toluene **7**. The trifluoroacetyl compound **7** was then reacted with hydroxylamine hydrochloride in pyridine to form oxime **8**. Reacting the latter with *p*-toluenesulfonyl chloride led to the tosylated oxime **9**, which was placed in a thick-walled screw-capped flask and reacted overnight with liquid ammonia in diethyl ether to form the diaziridine **10**; under dim red light, diaziridine **10** was oxidized with iodine to give methylphenyl-trifluoromethyl-diazirine **11**. Finally, **11** was brominated with *N*-bromosuccinimide (NBS) using a catalytic amount of 2,2'-azobisisobutyronitrile (AIBN) to form 3-(4-bromomethylphenyl)-3-trifluoromethyl-3*H*-diazirine (**12**, Scheme 1). Benzoyl peroxide was initially used as a radical initiator, but the reaction yielded multiple products resulting from multiple bromine substitutions. The use of AIBN led to a 4:1 ratio of monobrominated **12** and geminal dibromo-substituted methylphenyl-trifluoromethyldiazirine, but

Scheme 1^a



^a Reagents: (a) *N*-Trifluoroacetyl piperidine, *n*-butyllithium. (b) Hydroxylamine. (c) *p*-Toluenesulfonyl chloride, pyridine. (d) NH₃. (e) I₂, Et₃N. (f) NBS, AIBN. (g) NaN₃. (h) Me₂NHBH₃. (i) PBr₃.

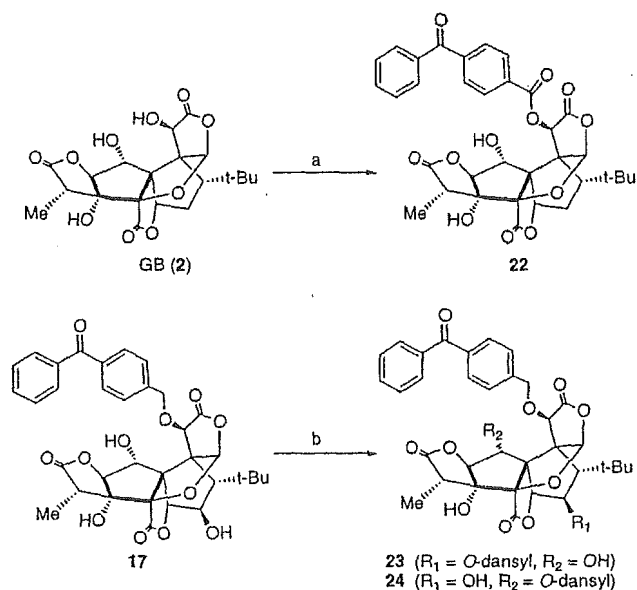
Scheme 2^a

^a Reagents: (a) 4-(Bromomethyl)benzophenone, KH. (b) Compound 12, KH. (c) Compound 15, KH.

separation of the two products required several repetitions of flash column chromatography to yield the monobromo-substituted diazirine 12 in sufficient purity.

For the synthesis of tetrafluorophenyl azide 15, pentafluorobenzaldehyde was heated with sodium azide in an acetone–water mixture. Because pentafluorophenyl groups that contain electron-withdrawing groups undergo nucleophilic aromatic substitution regioselectively in the para position, azidophenylaldehyde 13 was obtained in high yield, and no ortho-substituted product was observed. Aldehyde 13 was selectively reduced with a dimethylamine–borane complex to form the benzyl alcohol 14. The benzyl alcohol 14 was then brominated by refluxing with phosphorus tribromide in pyridine and chloroform to give the desired product 15 (Scheme 1).

Preparation of GB and GC derivatives 16–21 was performed by reacting GB (2) and GC (3) with 4-(bromomethyl)benzophenone, 3-(4-bromomethylphenyl)-3-trifluoromethyl-3*H*-diazirine (12), and 1-azido-4-(bromomethyl)-2,3,5,6-tetrafluorobenzene (15), respectively (Scheme 2). Ginkgolides GB (2) and GC (3) were derivatized almost exclusively at 10-OH when potassium hydride (KH) was used as base, as was previously shown for GB (2),⁴⁰ whereas other bases were less selective, giving rise to products derivatized at 1-OH as well. It is noteworthy that 7-OH present in GC (3) does not react under any of the above-mentioned reaction conditions. Generally, the position of the substituent was determined from the ¹H NMR coupling of appropriate protons in dimethyl sulfoxide (DMSO)-*d*₆, as well as by correlation spectroscopy (COSY) spectra. The

Scheme 3^a

^a Reagents: (a) 4-Benzoylbenzoic acid, EDC, DMAP. (b) Dansyl chloride, DMAP.

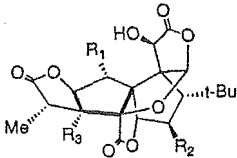
relative chemical shift of 12-H in DMSO-*d*₆ can also be used in differentiating 1- and 10-OH substitutions.⁴²

The coupling of GB (2) with 4-benzoylbenzoic acid using 1-[3-(dimethylamino)propyl]-3-ethylcarbodiimide HCl (EDC) and 4-(dimethylamino)pyridine (DMAP) occurred exclusively at 10-OH to give 10-benzophenonecarbonyl GB (22) in good yield (Scheme 3). In 10-benzophenonecarbonyl GB (22), the photoactivatable benzophenone moiety is linked to the ginkgolide skeleton through an ester linkage. After it is incorporated into the receptor, the ester group can be aminolyzed with a fluorescent amine such as 1-pyrenemethylamine, thus avoiding the use of radioactivity for photolabeling and sequencing.⁵⁴

GC derivatives 17, 19, and 21 can be reacted further to incorporate fluorescent groups; for example, benzophenone derivative 17 was reacted with 1 equiv of 5-(dimethylamino)naphthalene-sulfonyl (dansyl) chloride to give 10-*O*-benzophenone-7-*O*-dansyl GC (23) with almost exclusive reaction at 7-OH (Scheme 3). Interestingly, increasing the amount of dansyl chloride to 2 equiv gave 10-*O*-benzophenone-1-*O*-dansyl GC (24) as well as 23 in a 1:1 ratio.

All compounds were characterized by NMR spectroscopy and high-resolution mass spectrometry (HRMS). Purity of the derivatives 16–24, with aromatic groups, was determined by high-performance liquid chromatography (HPLC)–UV and ¹H NMR and was in the range of 98–100%. Because ginkgolides (1–5) and bilobalide (6) absorb only weakly in the UV spectrum, HPLC–UV cannot be used for determination of purity. Instead, observation of the 12-H ¹H NMR signal of 1–6 is a particularly useful way to determine purity, as this signal has distinct and well-separated δ -values for ginkgolides, bilobalide, and their derivatives.

Pharmacology. The native TTLs (1–6), as well as ginkgolide derivatives 16–24, were tested for their ability to bind to PAFR using a radioligand binding assay with membrane fractions from hearts and skeletal muscles of PAFR transgenic mice.⁵³ Initially, compounds were tested in concentrations of 5 μ M against [³H]WEB

Table 1. K_i Values of the Native TTLs


| compd | R ₁ | R ₂ | R ₃ | K_i (μM) ^a |
|----------------|----------------|----------------|----------------|--------------------------------------|
| GA (1) | H | H | OH | 1.46 |
| GB (2) | OH | H | OH | 0.56 |
| GC (3) | OH | OH | OH | 12.6 |
| GJ (4) | H | OH | OH | 9.90 |
| GM (5) | OH | OH | H | >50 |
| bilobalide (6) | | | | >50 |

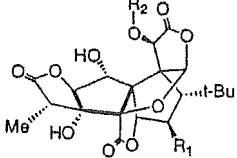
^a Inhibition of [³H]WEB 2086 binding. Values are means of two independent experiments performed in triplicate.

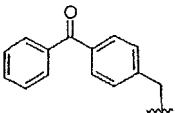
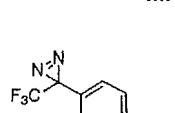
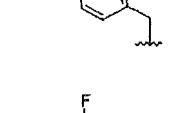
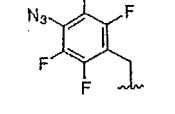
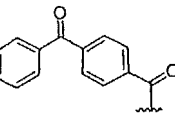
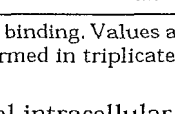
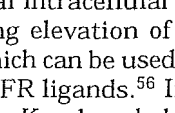
2086 (Figure 2), a potent, competitive PAFR antagonist and [³H]PAF; the compounds were generally less potent against [³H]PAF, but the relative potencies were comparable with the two radioligands. The degree of non-specific binding was determined to be ca. 50% for [³H]PAF and less than 5% for [³H]WEB 2086. Accordingly, the assays were performed using [³H]WEB 2086 rather than [³H]PAF as the radioligand, due to the high degree of nonspecific binding of the latter.

All compounds were dissolved in DMSO to obtain 5 mM stock solutions of test compounds. Examination of the effect of DMSO on the binding of [³H]WEB 2086 revealed that up to 1% DMSO (final concentration) was acceptable, but 1–2.5% resulted in a slight inhibition of [³H]WEB 2086 binding. Generally, this caused no problem; however, with very weakly binding compounds, the relatively high DMSO concentration in solutions above 100 μM had a small inhibitory effect, thus leading to a slight overestimation of their potencies. Previous studies have reported problems associated with the solubilization of ginkgolides specifically in DMSO,⁵⁵ but similar problems were not observed in the present study.

Native ginkgolides (1–5) and bilobalide (6) were tested with the cloned PAFR (Table 1). GB (2) was the most potent compound with a K_i value of 0.56 μM , while GA (1) was slightly less potent with a K_i of 1.46 μM . GC (3) and ginkgolide J (GJ, 4) were significantly less potent, while ginkgolide M (GM, 5) and bilobalide (6) both had K_i values larger than 50 μM .

The GB-derived photoactivatable compounds 16, 18, 20, and 22 with K_i values in the range 0.09–0.15 μM (Table 2) were all more potent than GB (2), while compounds 17, 19, and 21 derived from GC (3) with K_i values of 0.47–0.79 μM were equipotent to GB (2) (Table 2), despite the fact that GC (3) itself is only weakly potent. Besides proving that aromatic groups linked to 10-OH enhance activity in both GB (2) and GC (3) derivatives, these results also indicate that the specific type of photoactivatable group was less important. Derivatives 23 and 24 possessing a fluorescent dansyl group at either 1- or 7-OH were both less potent than 10-*O*-benzophenone GC (17) without the dansyl group, with K_i values of 3.94 and 0.96 μM for 23 and 24, respectively. However, an important difference was observed in the activities between the two; the 1- and 10-disubstituted analogue (24) was ca. four times more potent than the 7- and 10-disubstituted analogue (23).

Table 2. K_i Values of the Synthesized Derivatives


| compd | R ₁ | R ₂ | K_i (μM) ^a |
|-------|----------------|---|--------------------------------------|
| 16 | H |  | 0.15 |
| 17 | OH |  | 0.58 |
| 18 | H |  | 0.15 |
| 19 | OH |  | 0.47 |
| 20 | H |  | 0.09 |
| 21 | OH |  | 0.79 |
| 22 | H |  | 0.13 |

^a Inhibition of [³H]WEB 2086 binding. Values are means of two independent experiments performed in triplicate.

PAFR is linked to several intracellular signal transduction pathways including elevation of intracellular calcium concentration,²² which can be used for analyzing functional responses of PAFR ligands.⁵⁶ In the present study, the compounds with K_i values below 5 μM , i.e., GA (1), GB (2), and analogues 16–22, were investigated for their ability to mobilize intracellular calcium in Chinese hamster ovary (CHO) cells expressing the PAFR.⁵⁷ While none of them evoked calcium responses, they all suppressed PAF-induced intracellular calcium increase (data not shown) confirming their function as PAFR antagonists. Because the assay is based on the measurement of the fluorescence of a Ca^{2+} sensitive dye, the fluorescence of analogues 23 and 24 interfered with the measurement and could not be assayed.

Discussion

Nine analogues (16–24) with photoactivatable groups, and in the case of 23 and 24 with fluorescent dansyl groups as well, have been prepared from native ginkgolides GB (2) and GC (3) by selective derivatizations of the hydroxyl groups. Generally, the increased reactivity of the 1-OH and 10-OH as compared to 7-OH has been rationalized by stabilization of the corresponding alkoxides by hydrogen bonding between 1-OH and 10-OH,⁵⁸ but this does not explain the interesting selectivity for the 10-OH position in reactions with benzyl bromide derivatives. Notably, reaction of GC (3) with a bulky silyl chloride protection group occurs exclusively at the 1-OH of GC.⁵⁹ Three different photoactivatable moieties, all of them benzyl derivatives, were incorpo-

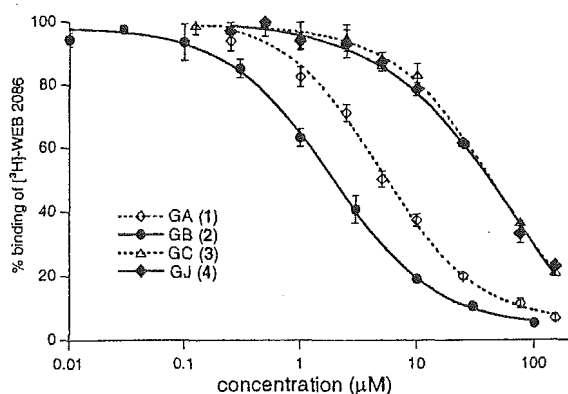


Figure 3. Concentration–displacement curves for native TTLs, as measured by their ability to displace binding of [³H]-WEB 2086 to the cloned PAFR. GB (2) was the most potent analogue, while GA (1) was slightly less potent, and GC (3) and GJ (4) were only weak antagonists. Bars represent the standard deviation (SD).

rated into both GB and GC. The benzophenone moiety was commercially available, whereas trifluoromethyl-diazirine **12** and tetrafluorophenyl azide **15** moieties were synthesized in six and three steps, respectively (Scheme 1). The three different types of photoactivatable groups were selected on the basis of their different reactive intermediates when irradiated, the intermediates being a radical, a carbene, and (singlet) nitrene for benzophenone, trifluoromethyl-diazirine, and tetrafluorophenyl azide, respectively.

All native TTLs (1–6) as well as the derivatized compounds were investigated with respect to their binding to cloned PAFR isolated from transgenic mice (Figure 3 and 4). To the best of our knowledge, this is the first report on the effect of TTLs on the cloned PAFR, since previous SAR studies of PAFR antagonism with TTLs and derivatives was performed by monitoring inhibition of PAF-induced rabbit platelet aggregation. GB (2) has generally been reported to be a potent antagonist of the PAFR based on the latter assay with an IC_{50} value around $0.2 \mu M$,^{40–42} which corresponds to the K_i value of $0.56 \mu M$ obtained in this study (Table 1). GA (1), with one hydroxyl group less than GB (2), was only slightly less potent than GB (2, Figure 3), indicating that the OH-1 is not essential for activity, and neither is the hydrogen bonding between OH-1 and OH-10. Generally, the binding of GC (3), GJ (4), and GM (5) with hydroxyl groups at C-7, as compared to the binding activity of GA (1) and GB (2) lacking the 7-OH, was decreased showing that the 7-OH is not necessary for binding to PAFR whereas hydroxyl groups at other positions appear to be less important (Figure 3). The study also confirmed that bilobalide (6), a TTL with only one five-membered carbocycle and three lactones, is not displacing [³H]WEB 2086 binding in concentrations up to $100 \mu M$ (Table 1).

All seven photoactivatable analogues **16–22** with aromatic substituents at 10-OH improved the affinity to the PAFR relative to the activities of GB (2) and GC (3) (Figure 4). This is in agreement with previous SAR studies of GB (2),^{40–42} as well as a three-dimensional (3D)-quantitative SAR (QSAR) study on ginkgolides.⁶⁰ However, it is interesting to note that aromatic substitutions at 10-OH of GC (3) as in compounds **17**, **19**, and **21** improve the affinity to PAFR ca. 20-fold thus making

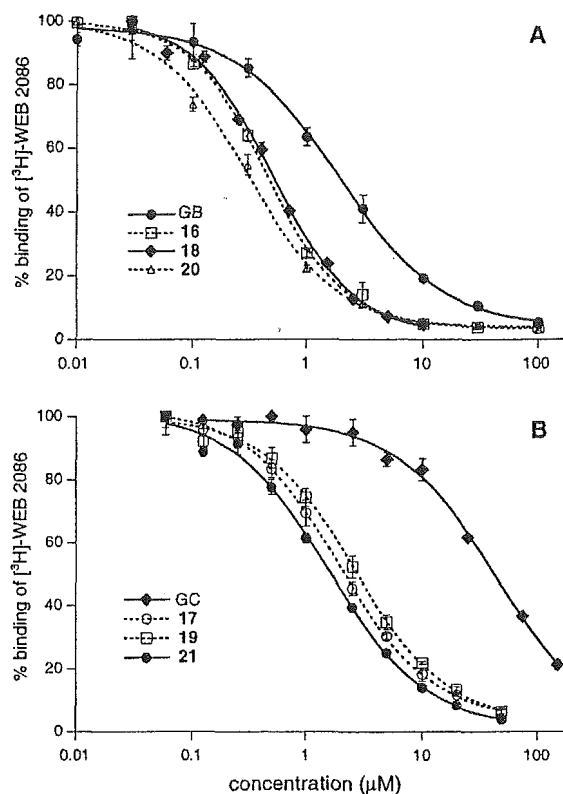


Figure 4. (A) GB (2) and photoactivatable benzyl derivatives; the three photoactivatable benzyl derivatives **16**, **18**, and **20** were all ca. 6-fold more potent than GB (2), and the activities were remarkably similar although bearing very different functional groups. (B) GC (3) and photoactivatable benzyl derivatives (**17**, **19**, and **21**) were all more potent than GC (3), with a remarkable increase in potency, thus being equipotent to GB (2). Bars represent the SD.

them equipotent to GB (2), while the same substitutions in GB (2) increase the affinity only 6-fold (Figure 4). Furthermore, the similar affinities of GB derivatives **16**, **18**, **20**, and **22** and the similar affinities of GC derivatives **17**, **19**, and **21** (Figure 4) imply that it is the steric bulk or the lipophilicity, including π – π interactions of the substituents, rather than the specific functional groups that are important for the increase in affinity.

GC derivatives **23** and **24** (Scheme 3) with dansyl groups at 7-OH and 1-OH are less potent and equipotent, respectively, to their parent compound, 10-*O*-benzophenone-GC (**17**). In compound **23**, which is ca. six times less active than **17**, the bulk at the 7-position seems to be responsible for the reduction in affinity. The fact that compound **24** is equipotent to **17** suggests that once a bulky aromatic group occupies this area, further aromatic groups neither increase nor decrease the affinity.

In conclusion, an investigation of the effect of TTLs isolated from *G. biloba* on the cloned PAFR has demonstrated that among the native compounds, GA (1) and GB (2) are the most potent. A series of photoactivatable analogues have been prepared, and PAFR binding assays showed that most of these analogues were more potent antagonists than their parent compounds, thus providing promising candidates for the planned studies of the interaction of ginkgolides with the PAFR. The ginkgolide derivative containing both a photoactivatable and a fluorescent group, compound **24**, retained affinity

to PAFR and thus could be useful in photolabeling and subsequent sequencing studies.

Experimental Section

Chemistry. General Procedures. Ginkgolides and bilobalide (**1–6**) were obtained by extraction of leaves from *G. biloba*, purification by column chromatography, and recrystallization, as previously described,^{3,61} and purity was >99% as determined by ¹H NMR. Solvents were dried by eluting through alumina columns. Triethylamine was freshly distilled from NaOH pellets. Unless otherwise noted, materials were obtained from a commercial supplier and were used without further purification. All reactions were performed in predried glassware under argon or nitrogen, and all reactions involving azides or diazirines were performed in dim red light. Flash column chromatography was performed using ICN silica gel (32–63 mesh) or ICN silica gel (32–63 mesh) impregnated with sodium acetate.⁶¹

Thin-layer chromatography (TLC) was carried out using precoated silica gel 60 F₂₅₄ plates with thickness of 0.25 μm. Spots were observed at 254 nm and by staining with acetic anhydride or cerium/molybdenum in H₂SO₄. ¹H and ¹³C NMR spectra were obtained on Bruker DMX 300 or Bruker DMX 400 MHz spectrometers and are reported in parts per million (ppm) relative to internal solvent signal, with coupling constants (*J*) in Hertz (Hz). For ¹⁹F NMR spectra, hexafluorobenzene (–162.9 ppm) was used as internal standard. Analytical HPLC was performed on a HP 1100 LC instrument using a 5 μm C18 reversed-phase Phenomenex Luna column (150 mm × 4.60 mm), using 1 mL/min of water/acetonitrile/TFA 60:40:0.1, raising to 50:50:0.1 after 10 min, and detecting by UV at 219 and 254 nm. Accurate mass determination was performed on a JEOL JMS-HX110/100A HF mass spectrometer using a 3-nitrobenzyl alcohol (NBA) matrix and Xe ionizing gas, and all are within ±5 ppm of theoretical values.

2,2,2-Trifluoro-1-(4-methylphenyl)-1-ethanone (7).⁴⁸ 4-Bromotoluene (9.45 g, 55.25 mmol) was dissolved in Et₂O (280 mL) and cooled to –40 °C. *n*-Butyllithium (1.1 M in hexane, 40.5 mL, 60.74 mmol) was added dropwise, and the solution was warmed to 0 °C over a 2 h period. The solution was then cooled to –60 °C and a solution of *N*-trifluoroacetyl piperidine⁴⁸ (10.00 g 55.23 mmol) in dry Et₂O (60 mL) was added in portions. The reaction was allowed to stir at –60 °C for 3 h and then warmed to room temperature. The solution was hydrolyzed with saturated NH₄Cl (50 mL) and washed with NH₄Cl (5 × 50 mL) and H₂O (3 × 50 mL). The organic phase was dried (MgSO₄), and the solvent was removed in vacuo. The remaining oil was purified by flash column chromatography eluting with hexane/CH₂Cl₂ (5:1, 4:1, and 3:1) to give a colorless oil (5.62 g, 54%). ¹H NMR (300 MHz, CDCl₃): δ 2.46 (s, 3H), 7.26–7.36 and 7.96–7.98 (AA'BB' system, 4H). ¹³C NMR (75 MHz, CDCl₃): δ 22.3, 117.0 (q, ¹J_{CF} = 292.5, CF₃), 127.9, 130.2 (2 C), 130.7 (2 C), 147.4, 169.1 (q, ²J_{CF} = 60.0).

2,2,2-Trifluoro-1-(4-methylphenyl)-1-ethanone Oxime (8).⁴⁸ Ketone **7** (2.60 g, 13.80 mmol) was dissolved in pyridine (30 mL), hydroxylamine hydrochloride (2.88 g, 41.44 mmol) was added, and the reaction was stirred at 70 °C for 3 h. Pyridine was removed in vacuo, and the remaining residue was dissolved in Et₂O (50 mL) and washed with 0.01 M HCl (50 mL). The organic layer was washed with H₂O (3 × 50 mL) and dried (MgSO₄), and the solvent was removed in vacuo to give a colorless solid (2.01 g, 72%), which was used without further purification. ¹H NMR (300 MHz, CDCl₃): δ 2.40 (s, 3H), 7.20–7.30 and 7.37–7.43 (m, 4H), 8.38 (bs, OH). Multiple splitting patterns arise due to anti/syn configurations of the oxime. ¹³C NMR (75 MHz, CDCl₃): δ 21.9, 121.0 (q, ¹J_{CF} = 277.5, CF₃), 123.4, 129.0 (2C), 129.7 (2C), 141.4, 148.4 (q, ²J_{CF} = 37.5).

2,2,2-Trifluoro-1-(4-methylphenyl)-1-ethanone *O*-(*p*-Toluenesulfonyl) Oxime (9).⁴⁸ To a stirred solution of oxime **8** (2.00 g, 9.85 mmol) in pyridine (36 mL), *p*-toluenesulfonyl chloride (2.82 g, 14.79 mmol) was added in portions and the reaction mixture was refluxed for 3 h. Pyridine was removed in vacuo, and the residue was purified by flash column

chromatography eluting with hexane/CH₂Cl₂ (2:1) to give a white solid (2.90 g, 82%). ¹H NMR (300 MHz, CDCl₃): δ 2.40 (s, 3H), 2.48 (s, 3H), 7.26–7.34 (m, 4H), 7.37–7.40 and 7.87–7.90 (AA'BB' system, tosyl aromatic H, 4H). ¹³C NMR (75 MHz, CDCl₃): δ 21.9, 22.2, 120.0 (q, ¹J_{CF} = 285.0, CF₃), 122.0, 128.9 (2C), 129.7 (2C), 129.9 (2C), 130.2 (2C), 132.0, 142.7, 146.4, 154.0 (q, ²J_{CF} = 67.5).

3-(4-Methylphenyl)-3-trifluoromethyldiaziridine (10).⁴⁸ In a thick-walled screw-cap tube, **9** (2.90 g, 8.12 mmol) was dissolved in Et₂O (20 mL). The solution was cooled to –78 °C, and liquid ammonia (3.5 mL) was added. The tube was screwed tightly, and the solution allowed rising to room temperature. The reaction was stirred for 12 h, and the solution was cooled to –78 °C. The cap was removed, and the mixture risen to room temperature to remove ammonia. The solution was partitioned between Et₂O (50 mL) and H₂O (50 mL), the organic layer was dried (MgSO₄), and the solvent was removed in vacuo. The product was purified by flash column chromatography eluting with chloroform to give a colorless solid (1.25 g, 77%). ¹H NMR (300 MHz, CDCl₃): δ 2.19 (NH, d, 1H), 2.38 (s, 3H), 2.74 (NH, d, 2H), 7.22–7.24 and 7.49–7.51 (AA'BB' system, 4H). ¹³C NMR (75 MHz, CDCl₃): δ 21.7, 57.9 (q, ²J_{CF} = 34.9), 125.0 (q, ¹J_{CF} = 278.7, CF₃), 129.3 (2C), 129.7 (2C), 130.1, 140.0.

3-(4-Methylphenyl)-3-trifluoromethyldiazirine (11).⁴⁸ Diaziridine **10** (1.25 g, 6.18 mmol) was dissolved in CH₂Cl₂ (25 mL), and triethylamine (2.58 mL, 18.54 mmol) was added and cooled to 0 °C. Iodine (1.73 g, 6.80 mmol) was added in small portions until a brown color persisted. The solution was washed with 1 M NaOH (25 mL), H₂O (25 mL), and brine (25 mL). The organic phase was dried (MgSO₄), and the solvent was carefully removed in vacuo at 20 °C due to volatility of the product. The crude product was purified by flash column chromatography eluting with hexane/CH₂Cl₂ (20:1) to give a colorless solid (1.03 g, 82%). ¹H NMR (300 MHz, CDCl₃): δ 2.36 (s, 3H), 7.07–7.10, 7.19 and 7.22 (AA'BB' system, 4H). ¹³C NMR (100 MHz, CDCl₃): δ 21.5, 28.9 (q, ²J_{CF} = 39.6), 123.0 (q, ¹J_{CF} = 274.7, CF₃), 125.5, 127.1 (2C), 130.8 (2C), 141.1.

3-(4-Bromomethylphenyl)-3-trifluoromethyldiazirine (12).⁴⁹ A solution of diazirine **11** (0.50 g, 2.50 mmol) in CCl₄ (10 mL) was heated to 70 °C and powdered NBS (0.66 g, 3.75 mmol) was added and stirred for 10 min, then AIBN (10 mg) was added, and the reaction was refluxed for 2 h. The precipitate was filtered, the solvent was removed in vacuo at 20 °C, and the crude product was purified by column chromatography eluting with hexane/CH₂Cl₂ (20:1) to give an oil (0.30 g, 40%). ¹H NMR (400 MHz, CDCl₃): δ 4.50 (s, 2H), 7.17–7.23, 7.43 and 7.47 (AA'BB' system, 4H). ¹³C NMR (100 MHz, CDCl₃): δ 28.3 (q, ²J_{CF} = 40.5), 39.7, 122.2 (q, ¹J_{CF} = 275.0, CF₃), 127.3 (2C), 129.6, 129.9 (2C), 139.8.

4-Azidotetrafluorobenzaldehyde (13).⁵⁰ To a solution of pentafluorobenzaldehyde (2.69 g, 13.72 mmol) in acetone (24 mL) and H₂O (9 mL), NaN₃ (1.06 g, 14.54 mmol) was added and the mixture was refluxed for 8 h. The solution was cooled to room temperature and diluted with H₂O (20 mL). The solution was extracted with ether (3 × 30 mL), the organic phase was dried (MgSO₄), and the solvent was removed in vacuo. The maroon-colored gum was sublimed at 70 °C under reduced pressure to give a colorless solid (1.80 g, 60%). ¹⁹F NMR (282 MHz, CDCl₃): δ –152.14 (m, 2F), –146.10 (m, 2F).

4-Azidotetrafluorobenzyl Alcohol (14).⁵⁰ 4-Azidotetrafluorobenzaldehyde (**13**, 1.80, 8.21 mmol) was dissolved in acetic acid (27 mL), and Me₂NH·BH₃ (0.58 g, 9.85 mmol) was added. The reaction was stirred at room temperature for 1 h. The acid versatiles were removed in vacuo at 45 °C. The residue was dissolved in CHCl₃ (10 mL) and washed with 5% Na₂CO₃ (3 × 10 mL). The organic phase was dried (MgSO₄), and the solvent was removed in vacuo to give a colorless solid (1.74 g, 97%), which was used without further purification. ¹H NMR (300 MHz, CDCl₃): δ 2.41 (OH, broad s, 1H), 4.79 (s, 2H). ¹⁹F NMR (282 MHz, CDCl₃): δ –150.90 (m, 2F), –143.75 (m, 2F).

1-Azido-4-(bromomethyl)-2,3,5,6-tetrafluorobenzene (15).^{51,52} Alcohol **14** (1.74 g, 7.93 mmol) was dissolved in a